Available online at www.sciencedirect.com
ScienceDirect
Journal of Catalysis 250 (2007) 19–24
JOURNAL OF CATALYSIS
www.elsevier.com/locate/jcat

# The impact of nitrogen mobility on the activity of zirconium oxynitride catalysts for ammonia decomposition

H. Soerijanto [a,b], C. Rödel [a], U. Wild [b], M. Lerch [a], R. Schomäcker [a], R. Schlögl [b], T. Ressler [a,*]

[a] *Technical University Berlin, Institute for Chemistry, Straße des 17. Juni 135, D-10623 Berlin, Germany*
[b] *Fritz-Haber-Institute of the MPG, Department of Inorganic Chemistry, Faradayweg 4-6, D-14195 Berlin, Germany*

Received 26 September 2006; revised 25 April 2007; accepted 28 April 2007

Available online 27 June 2007

**Abstract**

A zirconium oxynitride catalyst was used for the decomposition of ammonia to hydrogen and nitrogen. The onset of catalytic activity at ∼550 °C coincided with the onset of nitrogen ion mobility in the material and a phase change from the initial $\beta'$ phase ($\sim Zr_7O_{11}N_2$) to the nitrogen-rich $\beta''$ ZrON phase ($\sim Zr_7O_{9,5}N_3$). No hydrazine formation during an extended time on stream was detectable. Moreover, the onset of activity was also correlated to a rapid change in the electronic structure of the surface accompanying formation of the more active $\beta''$ ZrON phase. The results presented here show for the first time a direct correlation among the onset of ion conductivity as a bulk property, a modified electronic structure of the surface, and the catalytic performance of a heterogeneous catalyst.


*Keywords:* Ammonia decomposition; Zirconium oxynitrides; Heterogeneous catalysis; Structure activity relationship; Nitrogen conductivity

## 1. Introduction

Hydrogen is a promising candidate as a future energy carrier. However, the best way to store hydrogen for mobile applications remains under debate. In addition to physically stored hydrogen, small hydrogen-containing molecules can be used as hydrogen carriers in an on-board reforming process. Thus, methanol is often considered a suitable replacement for fossil fuels. However, the formation of carbon monoxide during the reforming process is a major disadvantage of using carbonaceous hydrogen storage molecules. Because CO acts as a fuel cell poison, it must be removed in downstream gas purification units, which reduces the overall efficiency of the reforming process. Moreover, steam reforming of carbonaceous hydrogen sources results in formation of the greenhouse gas carbon dioxide.

As a potential alternative to methanol, ammonia can be used as a hydrogen carrier [1]. Like methanol synthesis, ammonia synthesis is a large-scale industrial process that can be operated anywhere inexpensive hydrogen is available. The production of hydrogen by decomposition of ammonia is a particularly clean process that yields only hydrogen and nitrogen, which can be used in fuel cells without further purification. However, metal catalysts for ammonia decomposition may produce significant amounts of hydrazine [2]. Similar to carbon monoxide from methanol reforming, hydrazine formed from ammonia decomposition must be removed in a subsequent gas purification unit. The limited selectivity of common metal catalysts in ammonia decomposition originates from the presence of neighboring actives sites that facilitate hydrazine formation. Based on this assumption, we attempted to tailor the selectivity of an improved ammonia decomposition catalyst by rationally seeking new materials that avoid neighboring active sites. In contrast to metal catalysts, these materials should be able to provide nitrogen atoms from the catalyst bulk for the formation of dinitrogen molecules.

Nitrogen-conducting zirconium oxynitrides [3,4] are promising new ammonia decomposition catalysts that avoid the presence of neighboring metal sites. The combination of an appropriate intrinsic reactivity toward nitrogen and low reducibility make these materials promising candidates for ammonia cat-

* Corresponding author. Fax: +49 (0) 30 314 22106.
*E-mail address:* thorsten.ressler@tu-berlin.de (T. Ressler).

0021-9517/$ – see front matter 
doi:10.1016/j.jcat.2007.04.024

alysts. Here we describe first catalysis studies linking the catalytic behavior in the decomposition of ammonia to the onset of nitrogen mobility in the bulk of a zirconium oxynitride catalyst.

## 2. Experimental

### 2.1. Catalyst preparation

Zirconium oxynitride pellets were prepared from isostatically pressed commercial zirconia powder nitrided at 1900 °C in nitrogen atmosphere for 2 h (graphite resistance furnace), resulting in a mixture of nitrogen-free monoclinic $ZrO_2$ (m-$ZrO_2$) and the $\beta''$-type of zirconium oxynitride phase ($\sim Zr_7O_{9,5}N_3$) [9]. Subsequently, the material was quenched from a vertical tube furnace at 1300 °C (nitrogen atmosphere) in water. X-ray analysis after quenching showed a reduced amount of monoclinic zirconia and the metastable $\beta'$-phase of zirconium oxynitride ($\sim Zr_7O_{11}N_2$) [5]. For the catalysis testing described here, a sample composed of 51 wt% $ZrO_2$ and 49 wt% $\beta'$ ZrON phase was used (denoted as ZrON in what follows). Hot-gas extraction of the as-prepared material yielded a total amount of nitrogen of 1.63 wt% (theoretical, 1.62 wt%). After 3 months on stream during ammonia decomposition, the material exhibited a minor decrease in the amount of nitrogen (−0.30 wt%).

### 2.2. In situ X-ray diffraction

High-temperature X-ray diffraction (XRD) experiments were performed on a STOE STADIP diffractometer ($CuK\alpha_1$-radiation, $\lambda = 0.15406$ nm) equipped with a graphite resistance furnace. The oxynitride powders were filled into capillaries under nitrogen and heated at a rate of 20 K $min^{-1}$. At a given temperature, after an annealing time of 15 min, diffraction data were collected for 15 min using a position sensitive detector.

### 2.3. Catalyst testing

Catalysis measurements of the decomposition of ammonia ($NH_3 \rightarrow 0.5N_2 + 1.5H_2$, $\Delta H^0 = 46.2$ kJ/mol) were performed at atmospheric pressure in a plug-flow tube reactor (PFTR) from stainless steel (8 mm i.d.; height of catalyst bed, 5–15 mm) heated to the corresponding reaction temperature (Fig. 1). The temperature of the reactor was manually increased in steps of 20 K. Steady-state conversion was reached again after about 10 min. The conversion data reported here were determined after 20 min time on stream at the corresponding temperature.

The amount of ammonia and helium in the feed was adjusted by mass-flow controllers (Bronkhorst). This arrangement permits setting different ammonia partial pressures at different flow rates, resulting in different contact times. The mass-flow controller for ammonia needed a special seal and a reliable pressure reducer of particular precision to properly adjust small flow rates of ammonia. The PFTR reactor was mounted into a heating block (brass, 80 mm i.d., 150 mm long), equipped with six high-temperature 220-W heating cartridges and heated to the desired temperature. The heating block is prepared to accommodate three reactors, enabling measurements with three

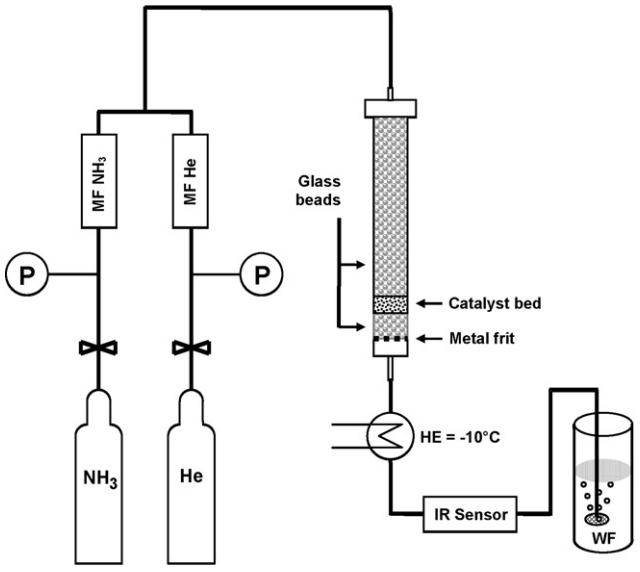


Fig. 1. Schematic arrangement of experimental setup: P = pressure reducer, MF = mass flow controller, HE = heat exchanger, WF = wash flask, filled with $H_2SO_4$.

catalysts under the same conditions within one test series. One reactor loaded with glass beads served as a blank reactor to determine the thermal and reactor contributions to the conversion of ammonia. The second reactor was filled with a conventional iron oxide-based catalyst (1 g $Fe_3O_4$ (magnetite) + 12.3 mg (1 mol%) $K_2CO_3$ + 18.2 mg (4 mol%) $Al_2O_3$, 0.3–1 mm particles, BET surface area ~7 $m^2/g$), which acted as a reference catalyst for ammonia synthesis. This catalyst was prepared in our lab as described previously [10]. The third reactor was filled with the zirconium oxynitride catalyst (4 g ZrON (0.3–1 mm particles, BET surface area ~0.9 $m^2/g$). The catalyst was tested as synthesized without further processing like pressing or crushing. Only the fraction of very fine particles was removed by sieving. The amount of catalyst used for testing was adjusted to yield comparable active surface areas. For the ZrON, the amount was limited by the size of the reactor. Glass beads were placed above and below the catalyst bed to ensure that the feed gases and the catalyst powder had the same preset temperature in the reaction zone.

To rule out diffusional limitations, the Weisz modulus, $\Psi'$, considering ammonia as the limiting reactant was estimated. The Weisz modulus describes the ratio of reaction rate to reactant diffusion rate and is defined by

$$\Psi' = L^2 \frac{m+1}{2} \frac{r_{\text{eff}} \rho_{\text{cat}}}{D_{\text{eff},NH_3} C_{NH_3}}, \tag{1}$$

where $L$ is the characteristic length of catalyst particle ($3 \times 10^{-4}$ m), $m$ is the reaction order of ammonia (1), $r_{\text{eff}}$ is the measured reaction rate ($2 \times 10^{-4}$ mol $s^{-1}$ $kg^{-1}$), $\rho$ is the catalyst density (6000 kg $m^{-3}$), $D_{\text{eff},NH_3}$ is the effective diffusivity of ammonia ($1 \times 10^{-6}$ $m^2$ $s^{-1}$), and $C_{NH_3}$ is the concentration of ammonia (0.14 mol $m^{-3}$).

With an effective rate of $2 \times 10^{-4}$ mol $s^{-1}$ $kg^{-1}$ estimated for 600 °C and the data given above, a Weisz modulus of 0.77 was calculated. This indicates that reaction proceeded slower

than diffusion of ammonia and that now mass-transfer limitations need to be considered neither at 600 °C nor at the lower temperatures.

The outlet gases were cooled to −10 °C to ensure that the product streams of different experiments were at the same temperature before reaching the ammonia sensor (Binos IR detector, Rosemount). Then the outlet gases were washed with sulfuric acid (1 L of washing liquid of 1 mol/L $H_2SO_4$). 4-(Dimethylamino)-benzaldehyde was added to test for hydrazine in the reaction product. Even after 2 weeks on stream, no hydrazine was detectable. During this time, 0.9 mol of ammonia was passed through the reactor. The detection limit for the hydrazine assay is 0.005 mg/L, which means formation of <0.4 ppm of hydrazine.

### 2.4. X-ray photoelectron spectroscopy

XPS measurements were performed in a modified LHS/SPECS EA200 MCD system equipped with facilities for XPS (Mg$K\alpha$ 1253.6 eV, 168 W power) and UPS (He I 21.22 eV, He II 40.82 eV). For the XPS measurements, a fixed analyzer pass energy of 48 eV was used, resulting in a resolution of 0.97 eV FWHM of the Ag $3d_{5/2}$ intensity. The binding energy scale was calibrated using Au $4f_{7/2} = 84.0$ eV and Cu $2p_{3/2} = 932.67$ eV. The base pressure of the UHV analysis chamber was $10^{-10}$ mbar. The ZrON catalyst was spread on a stainless steel sample holder as a uniformly distributed thin layer. At a given temperature of the sample holder (heating rate, 1 K/s), after an annealing time of 15 min, XPS data were collected for 10 min (only for O 1s and Zr 3d). Prolonged measurements of 90 min (for O 1s, N 1s, C 1s, and Zr 3d) were performed before and after the thermal treatment. Quantitative data analysis was performed by subtracting a Shirley background [11] and using empirical cross-sections [12].

## 3. Results and discussion

XRD patterns of the as-prepared material showed a mixture of monoclinic zirconia and the metastable $\beta'$-phase of zirconium oxynitride (~$Zr_7O_{11}N_2$) (Fig. 2). This material was used for catalysis testing and characterization and is referred to as ZrON. The conversion of ammonia as a function of temperature measured during ammonia decomposition on a conventional iron oxide-based catalyst (mostly $Fe_3O_4$), the ZrON catalyst (heating and cooling), and the blank reactor (glass beads) is depicted in Fig. 3. The iron oxide catalyst showed an onset of activity in the decomposition of ammonia at ~340 °C. Conversely, measurements of the as-prepared ZrON yielded no detectable activity below 550 °C. However, with further increases in reaction temperature, the zirconium oxynitride exhibited a jump in activity of ammonia decomposition at ~550 °C (Fig. 3). At reaction temperatures above ~550 °C, the activity of ZrON was similar to that of the conventional iron oxide-based catalyst. At temperatures above 600 °C, about 200 ppm of ammonia was still found in the effluent gas. This level of ammonia may be caused by a bypass of feed gas along the catalyst

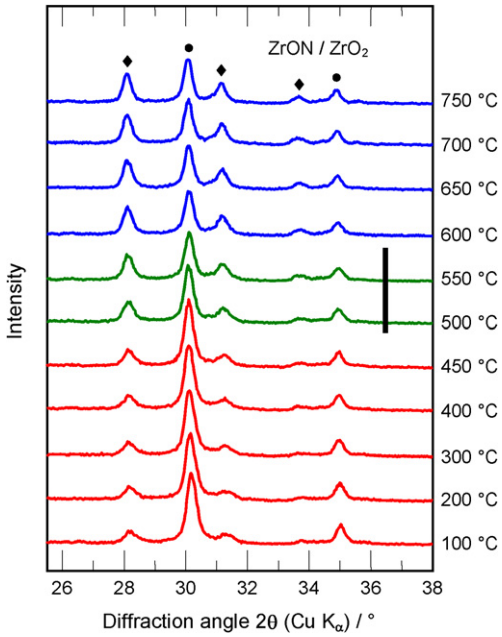


Fig. 2. Evolution of XRD patterns measured during thermal treatment of a mixture of zirconium oxynitride (●) and $ZrO_2$ (◆) in the temperature range from 100 to 750 °C. The phase change from the $\beta'$ ZrON phase to the $\beta''$ ZrON phase is indicated (bar).

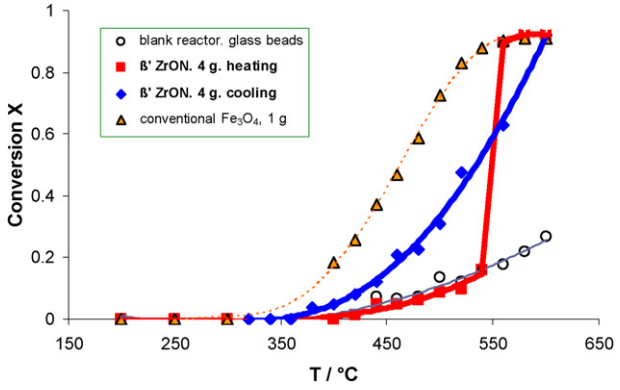


Fig. 3. Conversion of ammonia under steady state conditions as a function of temperature during ammonia decomposition over a conventional iron oxide based catalyst (open triangles) ZrON during heating (black squares) and cooling (black diamond) using a feed 50 ml STP/min He with 4100 ppm $NH_3$. A blank reactor experiment with glass beads (open cycles) is included.

bed, because the ratio of catalyst bed height (15 mm) to particle size (0.3–1 mm) did not meet the recommended value of 50 [13]. This bypassing of feed gas is also indicated by a weak asymmetry of the residence time distribution of the reactor. On cooling to ambient temperature, the ZrON catalyst showed a continuous decrease in ammonia conversion.

Compared with the conventional iron oxide-based catalyst, the sudden onset of catalytic activity of ZrON at ~550 °C does not correspond to a regular increase in activity with increasing reaction temperature. Because of the endothermic nature of the ammonia decomposition reaction, an ignition behavior of the reactor can be ruled out. Thus, rapid bulk structural changes must be assumed to be the origin of the catalytic activity observed. The high-temperature XRD data show that heating the

as-prepared metastable mixture of the nitrogen-poor $\beta'$-phase ($Zr_7O_{11}N_2$) and monoclinic $ZrO_2$ in nitrogen resulted in demixing to the nitrogen-rich $\beta''$-phase ($Zr_7O_{9.5}N_3$) and an increased amount of m-$ZrO_2$ at 550 °C (Fig. 3) [5]. The $\beta'$ and $\beta''$ phases can be described as anion-deficient fluorite structures. Whereas the $\beta'$ phase is strongly disordered, the $\beta''$ phase exhibits ordered anion vacancies [6,7]. Moreover, the $\beta''$ ZrON phase contains a larger amount of nitrogen ions in the lattice than the $\beta'$ phase, accompanied by an increased number of vacancies in the oxygen sublattice [7,8]. Apparently, phase demixing requires mobility of nitrogen ions in the ZrON structure to enable migration of nitrogen ions and the formation of $\beta''$ ZrON and $ZrO_2$. Therefore, the change from the $\beta'$ phase to the $\beta''$ ZrON phase is a suitable indicator for the onset of nitrogen ion conductivity in the ZrON catalyst studied.

The sudden onset of catalytic activity of ZrON in ammonia decomposition (Fig. 3) corresponds very well to the phase change from the initial $\beta'$ phase to $\beta''$ ZrON (Fig. 2). Apparently, the $\beta'$ phase exhibits only negligible activity in ammonia decomposition. Conversely, the $\beta''$ ZrON phase has considerable activity, similar to that of a conventional iron oxide-based catalyst. It can be envisaged that the $\beta''$ phase exhibits increased nitrogen mobility compared with the $\beta'$ phase, in addition to the increased amount of nitrogen in the $\beta''$ phase. Both of these properties may be prerequisites for the $\beta''$ phase to function as an active catalyst for ammonia decomposition. Thus, the reduced amount and mobility of nitrogen in the initial $\beta'$ phase is not sufficient to merit detectable catalytic activity.

XRD studies have shown that the $\beta''$ phase persists on cooling and does not change back to $\beta'$ ZrON [5]. This metastability of the $\beta''$ ZrON phase is nicely reflected in the conversion of ammonia during the cool-down period (Fig. 3). Even below the phase demixing temperature, the increased amount of nitrogen and its mobility in the $\beta''$ ZrON phase resulted in an improved activity compared with the $\beta'$ phase. Moreover, the ammonia conversion on $\beta''$ ZrON exhibited a more regular behavior as a function of the decreasing temperature. Subsequently increasing the temperature under reaction conditions resulted in a regular increase in activity of the catalyst that coincided with the cooling curve of the first temperature cycle.

To determine the apparent activation energy of ammonia decomposition on the ZrON catalyst used, the partial pressure of ammonia in the feed was varied, and the conversion of ammonia was determined as a function of temperature. The ammonia conversion on ZrON at a given temperature and residence time was independent of the ammonia partial pressure (Fig. 4). Apparently, the ZrON catalyst was not saturated under the applied conditions, and thus the results obtained for the initial conversion indicate a first-order reaction.

For a first-order reaction, the conversion of ammonia in a PFTR reactor can be described by $X = 1 - \exp((-c_{kat}k_{cat} + k_{uncat})\tau)$ with $X = (p_{NH_3,0} - p_{NH_3})/p_{NH_3,0}$. Assuming a temperature dependency of the rate constant according to the Arrhenius equation [$k = A\exp(-E_A/RT)$], the apparent activation energy $E_A$ can be determined by fitting the equation to the conversion data as a function of temperature (Fig. 4). The contribution of the blank reactor was taken into account by fitting $k_{uncat}$ and $E_{A,uncat}$ to the data obtained without catalyst. An apparent activation energy of 106 ± 10 kJ/mol was obtained at 400–550 °C. This value is in good agreement with activation energies assumed for ion conductivity in zirconium oxynitride-based materials. [3] For the uncatalyzed reaction, an activation energy of 70 ± 10 kJ/mol was calculated from the conversion data. Moreover, the apparent activation determined corresponds well with the expected and previously reported values of ∼120 kJ/mol [8]. On one hand, the similar activation energies indicate a similar rate-determining step of the reaction on ZrON and reduced metal catalysts. On the other hand, the absence of detectable amounts of hydrazine is indicative of a mechanism of ammonia decomposition on ZrON that varies from that of conventional reduced-metal catalysts. This corroborates the correlation between onset of catalytic activity and nitrogen mobility in the bulk of the ZrON catalyst as a new mechanistic concept for this class of materials. Details on the role of anion vacancies and anion mobility in the material for kinetics of the decomposition of ammonia will be further elucidated in future work.

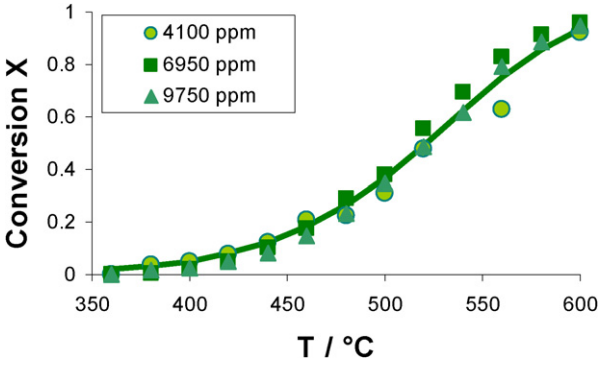


Fig. 4. Conversion of ammonia on 4 g ZrON measured at different concentrations of ammonia in the He flow of 50 ml STP/min. The solid line represents a refinement of a first-order reaction kinetics to the data obtained for 6950 ppm $NH_3$ in the feed of 50 ml STP/min. Within the series for 4100 ppm two data points are missing because of failing the ammonia detector. All measurements were taken during the cooling cycle.

In addition to bulk structural properties, the electronic structure of the surface of the ZrON catalyst as a function of temperature was studied by XPS. The Zr 3d doublet exhibited only minor changes in shape and position during heating and cooling (Fig. 5A); however, at ∼550 °C, an abrupt broadening and shift in binding energy of the Zr 3d peak appeared (Figs. 5B and 5C), possibly due to changes in differential charging of the surface. The corresponding change in the electronic structure of the ZrON catalyst coincided with the onset of catalytic activity (Fig. 3) and nitrogen ion mobility of $\beta''$ ZrON (Fig. 2). Subsequently, the resulting surface structure of the $\beta''$ ZrON phase persists (Fig. 5) and retains its catalytic activity even at temperatures below 550 °C (Fig. 3). Moreover, a quantitative analysis of the XPS data revealed an increasing amount of nitrogen at the surface of the ZrON material after heating to 600 °C (Table 1).

Apparently, the dynamic behavior of the surface of the ZrON catalyst under reaction conditions accompanies the phase change in the ZrON material at ∼550 °C. Thus, the formation

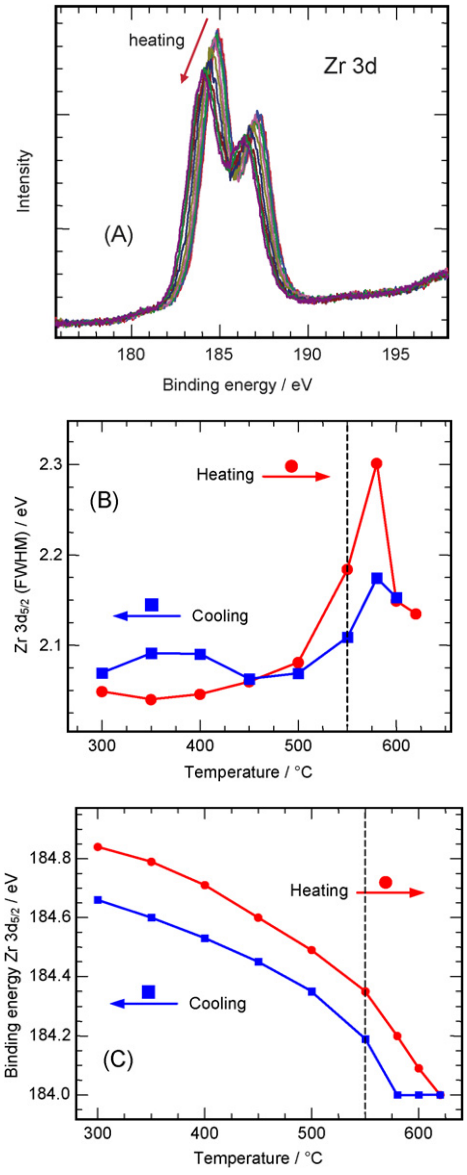


Fig. 5. Evolution of XPS Zr 3d peak of $\beta'$ ZrON (A), Zr $3d_{5/2}$ peak width (FWHM) (B), and binding energy (C) during heating and subsequent cooling. The dashed line in (B) and (C) indicates the onset of the phase change from $\beta'$ ZrON to $\beta''$ ZrON and catalytic activity.

Table 1
Surface composition (atom%) of ZrON material obtained from XPS measurements (O 1s, N 1s, Zr 3d) before (u) and after (d) thermal treatment between 200 and 620 °C

| Temperature | O (atom%) | N (atom%) | Zr (atom%) | O/Zr | O/N |
|---|---|---|---|---|---|
| 200 °C (u) | 55.02 | 6.02 | 21.83 | 2.52 | 9.14 |
| 620 °C | 55.5 | 7.9[a] | 24.1 | 2.3 | 7.0 |
| 200 °C (d) | 50.8 | 7.0 | 23.1 | 2.2 | 7.2 |

[a] Measured at 600 °C.

of the nitrogen-rich $\beta''$ ZrON phase is especially detectable at the surface, whereas the overall concentration of nitrogen in the bulk decreases only slightly during time on stream. This confirms the assumption of nitrogen mobility and $\beta''$ phase formation as prerequisites for activity of ZrON in ammonia decomposition. Apparently, the phase change from $\beta'$ to $\beta''$

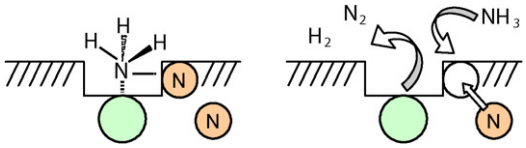


Fig. 6. Schematic representation of the decomposition of ammonia on a zirconium oxynitride catalyst.

phase results in the formation of characteristic lattice defects at the surface of the catalyst. In a corresponding schematic mechanism (Fig. 6), these defects are the active sites for the dissociative adsorption of ammonia. Subsequently, a dinitrogen molecule is formed together with a nitrogen atom from the lattice of the ZrON catalyst. Finally, the vacancy in the nitrogen sublattice thus generated is replenished by nitrogen diffusion from the bulk or ammonia from the gas phase (Fig. 6).

## 4. Conclusion

In summary, the zirconium oxynitride studied here showed significant catalytic activity in the decomposition of ammonia. The ZrON catalyst exhibited no formation of hydrazine during extended time on stream. The sudden increase in activity at ~550 °C coincides with the onset of nitrogen ion mobility in the material and the phase change from the initial $\beta'$ phase to the nitrogen-rich $\beta''$ ZrON phase. Moreover, an apparent activation energy of $106 \pm 10$ kJ/mol agrees well with the activation energy of ion conductivity in zirconia-based materials. The dramatic change in activity is also correlated with a rapid change in the electronic structure of the surface that accompanies the formation of the more active $\beta''$ ZrON phase. The results presented show here for the first time direct correlations among the onset of ion conductivity as a bulk property, a modified electronic structure of the surface, and the catalytic performance of a heterogeneous catalyst.

## Acknowledgments

Financial support from the Deutsche Forschungsgemeinschaft, DFG (LE 781/9-1, SCHL 332/6-1), is gratefully acknowledged.

## References

[1] (a) S.F. Yin, B.Q. Xu, X.P. Zhou, C.T. Au, Appl. Catal. A Gen. 277 (2004) 1–9;
(b) T.V. Choudhary, C. Sivadinarayana, D.W. Goodmann, Chem. Eng. J. 93 (2003) 69–80.
[2] G. Ramis, L. Yi, G. Busca, M. Turco, E. Kotur, R.J. Willey, J. Catal. 157 (1995) 523–535.
[3] J. Wendel, M. Lerch, W. Laqua, J. Solid State Chem. 142 (1999) 163–167.
[4] M. Kilo, A.M. Taylor, C. Argirusis, G. Borchardt, M. Lerch, O. Kaitasov, B. Lesage, Phys. Chem. Chem. Phys. 6 (13) (2004) 3645–3649.
[5] M. Lerch, O. Rahäuser, J. Mater. Sci. 32 (1997) 1357–1363.
[6] A.T. Tham, C. Rödel, M. Lerch, D. Wang, D.S. Su, A. Klein-Hoffman, R. Schlögl, Cryst. Res. Technol. 39 (5) (2004) 421–428.
[7] A.T. Tham, C. Rödel, M. Lerch, D.S. Su, A. Klein-Hoffman, R. Schlögl, Cryst. Res. Technol. 40 (3) (2005) 193–198.
[8] G. Papapolymerou, V. Bontozoglou, J. Mol. Catal. 120 (1997) 165.
[9] M. Lerch, J. Am. Ceram. Soc. 79 (10) (1996) 2641–2644.

[10] H. Bakemeier, H. Grössling, R. Krabetz, BASF Aktiengesellschaft Ludwigshafen, Ullmans Encyklopädie der technischen Chemie, 1973, pp. 444–513, Band 7.
[11] D.A. Shirley, Phys. Rev. B 5 (12) (1972) 4709–4714.
[12] D. Briggs, M.P. Seah, Practical Surface Analysis by Auger and X-ray Photoelectron Spectroscopy, vol. 1, second ed., Wiley, New York, 1990, pp. 635–638 (Appendix 6).
[13] R.O. Idem, N.N. Bakhshi, Chem. Eng. Sci. 51 (1996) 3697.